In order to maintain the competitive advantage of the medium short take-off and landing transport aircraft, the task must be solved of ensuring take-off and landing on the ground runways with a length of 600–800 m when installing a turbojet engine.

When the engines are installed on the pylons under the wing, this is achieved by using a «forced» turn of the jet of engines when the flaps are released at an angle of 60°. We have found the mutual location of the wing and the engine on its stagger, based on the position relative to the construction plane of the wing and the angle of installation. A reciprocal arrangement has been determined, making it possible to maximize the lift force owing to the turn of the jet stream. It has been shown that this achieves the continuous flow around the sections of the flaps when they are deflected at a 60-degree angle.

We have analyzed the temperature effect of the jet stream on the mechanization and the aircraft wing at the stages of take-off and landing at different positions of engines under the wing, at different flight speeds and angles of attack. The effect of mechanization on the distribution of jet stream speeds and temperatures has been analyzed. It is shown that decreasing the distance between the engine nozzle and the lower surface of the wing leads to an increase in the angle of the jet stream deviation. We have identified those tail section zones of the flap, which require special execution to operate at temperatures above 400 °C.

The impact of the jet stream on aircraft's drag in the cruising configuration has been analyzed, as well as the scheme of engine arrangement on the aircraft's electrically dependent systems. We have shown the absence of the impact of the jet stream on the aircraft's drag in the cruising configuration, the reduction of fuel consumption at cruising modes, as well as the favorable impact exerted on the electrically dependent systems due to the significant reduction of gas-dynamic losses along the power plant tract.

Ways to modernize the transport aircraft type of An-70 have been proposed to ensure its superiority in its class

Keywords: transport aircraft, turbojet twin-contour engine, jet stream turn, short takeoff

UDC 629.7.01
DOI: 10.15587/1729-4061.2020.208639

SELECTING THE MUTUAL ARRANGEMENT OF THE ENGINE AND WING IN A TRANSPORT AIRCRAFT FOR SHORT TAKE-OFF AND LANDING

V. Kudryavtsev
Head of Department*
E-mail: kudryavtsev@antonov.com
B. Strigun
Deputy Head of Department*
E-mail: strigun@antonov.com
V. Shmyrov
PhD, Vice President*
E-mail: shmyrov@antonov.com
V. Loginov
Doctor of Technical Sciences, Senior Researcher
Department of Aircraft Engine Design
National Aerospace University
«Kharkiv Aviation Institute»
Chkalova str., 17, Kharkiv, Ukraine, 61070
E-mail: flightpropulsion@gmail.com
*Antonov State Enterprise
Tupolieva str., 1, Kyiv, Ukraine, 03062

Received date 30.03.2020
Accepted date 14.07.2020
Published date 17.08.2020

1. Introduction

The scientific and technological advances accumulated in the research and development of short take-off and landing aircraft (STLA) may be used to address the challenge of developing aircraft with improved take-off and landing characteristics (TLCs) that are relevant to transport aviation. It is known that in many countries more than 30 % of the cargo flow is delivered along the lines that exploit airfields with a runway length (RW) of about 700–1,500 m. Therefore, the use of transport aircraft at these lines could significantly increase the efficiency of air transportation. Expanding the scope of the aircraft's possible utilization leads to an increase in the number of aircraft sold in the market, which also affects the cost of the aircraft and its competitiveness.

In recent years, ICAO has tightened aircraft requirements [1]. The development of aviation technology is on the way to reducing acoustic emission and significantly reducing the level of harmful emissions from the engine. However, despite the significant shortcomings of modern aircraft with GTE (gas turbine engine), interest in STLA is not waning. This is because the use of STLA saves the time of delivery of passengers and cargo between airports. Moreover, at present, owing to the use of more advanced engines as part of the powerplant (PP), as well as increased STLA cruising speed, the scope of their application in terms of flight range can also be expanded.

The construction of STLA is also an urgent task for military aviation. According to many experts, one of the main new properties that a combat aircraft of the 21st century will possess is to ensure the take-off and landing on damaged airstrips and shorter fields, which was proven in recent wars. This has recently been confirmed by intensive research in the analysis and development of effective means of reducing the runway and landing distances. Therefore, the improvement of transport aircraft TLCs based on the mutual arrangement of the engine and wing is one of the most relevant areas of scientific and technical research in aviation.

2. Literature review and problem statement

As one knows [2], in order to maintain the competitive advantage of the medium transport STLA, it is necessary to solve the task of ensuring the take-off and landing on the ground runways of 600–800 m when installing a turbojet twin-contour engine (TJTE). However, a comprehensive approach to research needs to be presented in justifying and addressing such challenges. Paper [3] indicates that one of the key roles in designing and upgrading the STLA design is the aerodynamic layout of the airframe that determines the drag, lift force, which affects the type of engine, the weight of the payload, and the flight range [3]. However, the authors did not show a way to ensure and implement these conflicting requirements.

The choice of layout should take into consideration the mutual location of the main elements of the fuselage, wing, appendage, engines, and other elements and systems. For the rational layout, by using a multi-factor analysis, work [4] applied methods of multidisciplinary optimization. However, the reported results cannot be applied to most layout schemes. The reason for this is the narrow ranges of the parameters and characteristics for optimization. The optimization of unconventional aerodynamic layouts of aircraft is addressed, for example, in study [5]. At the same time, the issues of gas-dynamic and aerodynamic integration of elements of the plane's airframe and its engines remain unsolved.

Paper [6] explores ways to reduce the fuel consumption required for the aircraft. Separate studies [7, 8] are carried out not only in the area of engine arrangement rationality to minimize power costs and create efficient thrust but also regarding the influence on the structure aeroelasticity. However, the cited studies do not take into consideration the temperature stresses on the structure in the region of flaps over the entire range of a flight cycle. This assumption does not take into account the resource characteristics of wing elements.

In a series of works [9–11], the aircraft's existing airframe structures obtained during aerodynamic design are being optimized. This takes into consideration the location of the pylon and the spatial orientation of the engine nacelle, which affects the aerodynamic circuitry of the aircraft. However, the cited works do not account for the effect of the temperature of the gas jet on the elements of the airframe. This does not allow for a comprehensive assessment of the proper mutual location of the aircraft airframe elements.

Several papers consider the location of the nacelle with the engine in line with a classic scheme – on the pylon under the wing [12, 13] or fuselage [14], and unconventionally – over the wing [15]. In optimizing the aircraft's existing layouts, the distribution of loads and total characteristics, the interaction between the jet of gas outflowing from the engine nozzle and the pylon and flap [16], the flow conditions in the vicinity of the nacelle, pylon, and wing at cruising flight mode are considered. However, these papers do not take into consideration variable temperature loads that affect the resource of airframe elements.

The authors of works [17, 18] compare different variants of the shape of the nacelle, for example, with the preliminary braking of the incoming flow in front of the air intakes. The change in the aircraft's total aerodynamic characteristics is analyzed depending on the shape of the fuselage and the end surfaces of the wing. At the same time, there is no single method for obtaining a technical solution on the rational layout of the nacelle and the wing of the aircraft.

It should be noted that the authors of papers [19, 20] consider the layout within the entire aircraft structure aerodynamics. When the tasks of local aerodynamics and various design issues are tackled, the engines themselves, the elements of wing mechanization, the end sections of the wing are often considered in isolation from the overall layout. This applies to solving the tasks of improving the efficiency of wing mechanization elements and ensuring the predefined level of carrier properties [21], improving aerodynamic characteristics, such as creating «solid» flaps [22]. However, obtaining this workflow efficiency is inherent in only one flight mode of an aircraft or engine operation. There is a need to study all areas of flight and the features of the workflow in the region of engine nozzle arrangement under the wing of the aircraft.

Thus, scientific and technical research on the choice of the mutual arrangement of the engine and the wing of transport STLA is timely for the modernization of existing aircraft models.

3. The aim and objectives of the study

The aim of this study is to substantiate the mutual location of the system «wing+released flap+powerplant» of a transport STLA to improve flight characteristics under a short takeoff and landing mode.

To accomplish the aim, the following tasks have been set:

– to analyze the basic requirements for the flight characteristics of a short take-off and landing aircraft;

– to justify the characteristics of a transport aircraft and compare them with European projects;

– to conduct a comprehensive study of the effects exerted by the jets of operating simulators on the aerodynamic characteristics of the mechanized model of the aircraft;

– to investigate the effect of the temperature of the TJTE jet stream on the wing and mechanization.

4. Studying the flight and technical characteristics of a short take-off and landing aircraft

4. 1. Basic requirements for the flight characteristics of a short take-off and landing aircraft

Requirements for the take-off and landing characteristics, cargo transportation, and cruising speeds predetermine a new approach to the design proposal of a short take-off and landing aircraft with turbojet engines and the increased bypass ratio m=8–10.

To operate from the ground runways that are 600–800 m long, in order to provide for a speed reserve of $1.2 \cdot V_{SR}$ (V_{SR} is the stall speed), the landing speed must equal 190–200 km/h. This ensures control over the planning glissade to land the

aircraft accurately with a margin of landing length of no more than 100 m. Under all conditions, the following flight and technical requirements must be met:

– the transportation of 20 tons of cargo from the ground runways for a short take-off and landing range of 3,000 km;

– the cruising speed is 750–800 km/h.

The aircraft must climb and land on steep trajectories and take off with one engine failed from unpaved airfields.

According to the requirements for STLA, the main feature of the aircraft is its ability to take off and land with short run and mileage, the possibility of operating as a transport aircraft under the mode of standard takeoff and landing.

To meet these requirements, a powerful system is needed for intensive blowing by gas-air jets from the engines of the mechanized wing to increase the lift force of the aircraft. At the same time, there should be a good performance of the aircraft at low flight speeds and the necessary level of aerodynamic quality at cruising modes. When operating an aircraft from the ground runways, all requirements for the reliability of the aircraft's elements should be met.

In order to reach a compromise on specific fuel costs, we consider an aircraft with the wing sweep of $\chi_{1/4}=14–20°$ at an elongation of $\lambda=9–10$. A wing with this lengthening may be optimal in weight for the case of applying supercritical profiles. For supercritical profiles, a characteristic feature is the even distribution of lift force along the chord in the absence of «pressure peaks» in the tip of wing profiles [23]. A wing based on the supercritical profiles makes it possible to increase the speed of flight, at which there is a sharp increase in drag as a result of the formation of supersonic zones and shock waves, leading to spikes in pressure, density, and temperature.

4. 2. Comparative characteristics of the transport aircraft with European projects

A project of a transport aircraft with TJTE (Fig. 1) has been selected for the estimation study.

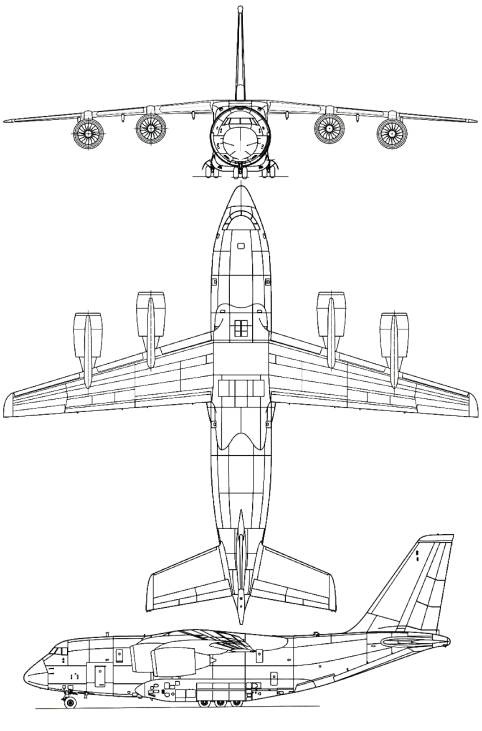

Fig. 1. General view of the transport aircraft project with TJTE

The goal of designing a new competitive aircraft or modernizing it is to achieve new improved performance characteristics of the aircraft, in particular, flight and technical data [2, 23].

The medium transport aircraft with TJTE is a model aircraft, unique in terms of its operational characteristics. The basic characteristics of the project of the domestic transport aircraft with TJTE are given in Table 1. This aircraft project enables direct delivery of cargo and equipment for short, 600–800 m long, poorly prepared ground airfields with a ground strength up to 0.588 MPa (6 kgf/cm^2). Under a short take-off and landing mode, 20 tons of cargo are transported over a flight range of L_{flight}=3,370 km. However, for the variant of standard take-off and landing, the aircraft can carry 47 tons of cargo over a flight range of L_{flight}=2,720 km, which allows it to perform the tasks for aircraft of significantly larger dimensions. According to these indicators, it significantly exceeds the capacity of the similar European aircraft A400M [24], which can be operated from airfields no shorter than 915 m and lift cargo no more than 37 tons.

Table 1

Basic flight technical characteristics of the transport aircraft with TJTE

Application mode	Standard take-off and landing mode	Short take-off and landing mode
RW required length, m	1,900	600–800
Take-off mass, t	145	118
Cargo capacity, t: – overload; – maximal; – estimated	 47 35 20	 – – 20
Cruise speed, km/h	750–800	
Cruising altitude, km	9.45–12.0	
Practical range with cargo, km: – 47 t; – 35 t; – 20 t; – no cargo	 2,720 4,700 6,300 7,370	 – – 3,370 –
Fuel efficiency, g/t·km	155	

The aircraft's project allows the high-precision landing of military cargoes, including mono-loads weighing up to 21 tons, which exceeds the capabilities of the Il-76 family of aircraft and the European A400M family and is approaching the capabilities of the heavy transport aircraft S-17, which has twice the takeoff weight and three times the price.

Given its dimensions and take-off mass, the medium transport aircraft with TJTE approaches the European Airbus Military A400M aircraft; moreover, significantly exceeds it in terms of basic flight-technical characteristics (Table 2).

To achieve a high technical level, the aircraft is equipped with the developed unique aerodynamic layout of the powerplant and the highly mechanized wing, which makes it possible to generate a very high lift force, necessary for the short take-off and landing.

The weight perfection of the military transport aircraft with TJTE is ensured by the rational design and wide use of modern metallic and composite materials. Composite materials are used to manufacture such elements of the structure as the vertical and horizontal appendage, wing mechanization, the wing and chassis fairings, as well as cargo hatch doors.

Table 2

Comparative characteristics of the domestic military transport aircraft with TJTE and A-400M

Characteristic	Transport aircraft with TJTE	A400M	Difference
Cargo cabin volume, m^3	370	356	4 %
Maximum payload, t	47	37	27 %
Minimum runway length under a short take-off and landing mode, m	600–800	915	34–14 %
Maximum payload under a short take-off and landing mode (runway of 915 m), t	35	20	42 %
Flight range under a short take-off and landing mode (runway of 915 m) with a cargo of 20 tons, km	4,900	2,000	59 %
Flight range with a cargo of 37 tons, km	4,700	3,700	22 %

The aircraft is equipped with a set of equipment to ensure the loading and unloading of cargo outside the base, as well as an autonomous onboard maintenance system.

Below are the tasks that are to be solved during a deep modernization of the transport aircraft:

1) reduce noise on the ground (as only the requirements of Chapter 3 of ICAO Annex 16 are met) [1];

2) reduce the loss of total pressure at the input to the engine [25];

3) reduce service time;

4) reduce the power consumed by the aircraft;

5) expand the ability of air intake from an engine compressor;

6) ensure the inclination angle of the ramp and sub-cranes in the position for loading (unloading) the equipment – 12°;

7) install the doors for landing personnel in the tail of the aircraft.

To ensure the implementation of tasks related to deep modernization, it is planned to install on the pylons under the wing four turbojet twin-contour engines CFM Leap produced by CFM International (Fig. 2), enabling the blowing of the flaps [23, 26]. The choice of new propulsion engines was based on the maximum possible identity of their weight and traction characteristics with the original PP with the preservation of the set of flight-technical characteristics. This provides flutter characteristics at high flight speeds and the characteristics of short take-off and landing not lower than those of the aircraft with TJTE.

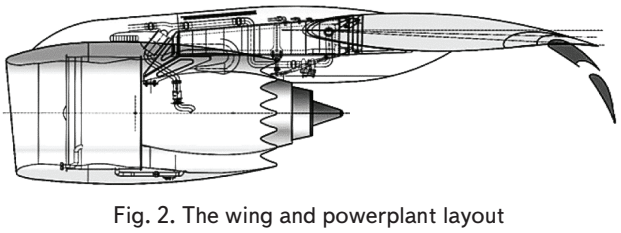

Fig. 2. The wing and powerplant layout

Replacing the propulsion powerplant provides the following benefits:

– the possibility to provide for noise on the ground under chapter IV of ICAO;

– increased comfort to the crew in the cargo cabin – noise less than 80 dB;

– the possibility to increase the airframe and system resource by reducing vibration and acoustic loads;

– the possibility to obtain more selected air for the heating of wing and appendage surfaces;

– the possibility to improve aerodynamic quality in the cruising configuration by reducing the area of the nacelle midline;

– the possibility of obtaining a more acceptable balance of the aircraft;

– the laborious maintenance and repair of the propulsion powerplant and systems is reduced by 30–35 %;

– the possibility of reducing radar visibility.

5. Comprehensive study into the patterns of the impact of jets from working simulators on the aerodynamic characteristics of the mechanized model of the aircraft

In order to ensure the implementation of the project of a short take-off and landing transport aircraft with a high bypass ratio (m=8–10), we have performed comprehensive studies into the patterns of the impact of the jets from working simulators on the aerodynamic characteristics of the mechanized model of the aircraft. The model used was a model of the An-77 aircraft with an elongated wing of λ=9.5, a narrowing of η=3.45, and a sweep angle of $\chi_{1/4}$=14°. At the place of installation of the attached simulators of turbofan engines D-227 with SV-227 propellers, four attached simulators of TJTE with air turbines were installed. The simulators were mounted on the relative wingspans of 0.383 and 0.65, and the turbines were powered by compressed high-pressure air.

In order to optimize the position of the engines on the influence of the engine stagger along the wing chord, as well as the position for the height and the wedged angle of the engine relative to the local wing chord, we analyzed modern layouts of PPs on the pylons under the wing of the aircraft. The region of engine arrangement for parametric research in the wind tunnel was determined.

Fig. 3, 4 show the parameters for installing the engine simulators. The parameters are recorded as follows:

– $\bar{X}_{nozzle} = X_{nozzle}/b_{section}$ – a nozzle extension relative to the wing profile tip in the cross-section of engine installation along the construction plane of the wing;

– $\bar{Y}_{axis} = X_{axis}/b_{section}$ – a position of the engine axis relative to the plane parallel to the construction plane of the wing, drawn through the tip of the profile of the cross-section of engine installation;

– $\phi_{install}$ – an angle between the engine axis and the line parallel to the construction plane of the wing.

The values of these parameters for different versions of the studies are given in Tables 3–5.

Our studies have shown that when increasing the traction coefficient of the TJTE simulator the blowing of the flaps with jets leads to a significant increase in the carrying abilities of the wing due to the deviation of the jet. This restores the continuous streamlining of the mechanization of the rear edge of the wing and increases the super-circulation around the wing.

The greatest increment of the lift force is achieved by deflecting the flaps at large angles (δ_{flap}=60°) at the closest position of the nozzles to the wing.

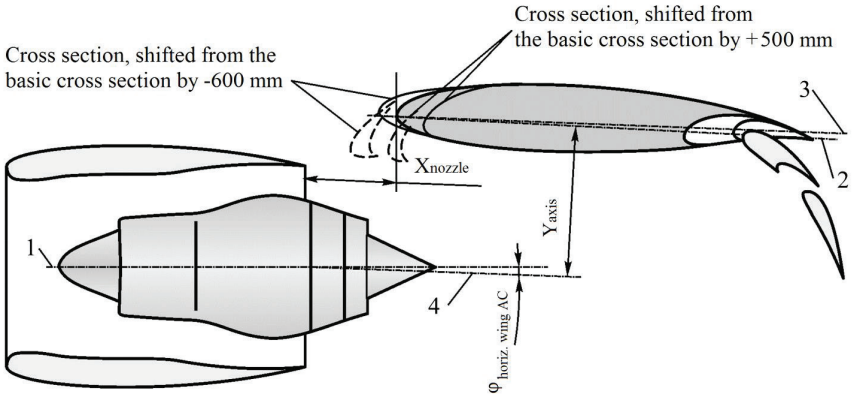

Fig. 3. Parameters for installing the simulators of internal engines:
1 — engine axis; 2 — construction plane of the wing; 3 — wing chord in the cross-section of engine installation;
4 — line parallel to the construction plane of the wing

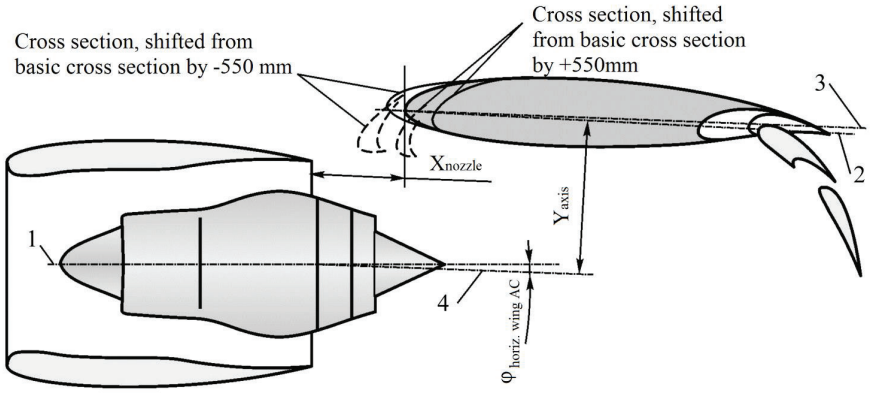

Fig. 4. Parameters for installing the simulators of external engines:
1 — engine axis; 2 — construction plane of the wing; 3 — wing chord in the cross-section of engine installation;
4 — line parallel to the construction plane of the wing

Table 3

Parameters for installing engine simulators for different examined variants

Variant No.	Wing cross-section on relative span 0.383				Wing cross-section on relative span 0.65			
	$\bar{X}_{nozzle}$	$\bar{Y}_{axis}$	$\phi_{install}$, degrees	$\beta_{nacelle}$, degrees	$\bar{X}_{nozzle}$	$\bar{Y}_{axis}$	$\phi_{install}$, degrees	$\beta_{nacelle}$, degrees
1	−0.22	−0.29	0	0	−0.267	−0.357	−1.5	0
1a	−0.22	−0.29	−1.5	0	−0.267	−0.357	−3.0	0
2	−0.22	−0.32	−1.5	0	−0.267	−0.393	−3.0	0
3	−0.22	−0.26	−1.5	0	−0.267	−0.32	−3.0	0
4	−0.22	−0.237	+1.5	0	−0.267	−0.32	+1.5	0
5	−0.26	−0.29	−1.5	0	−0.32	−0.357	−3.0	0
6	−0.18	−0.29	−1.5	0	−0.218	−0.357	−3.0	0

Table 4

Parameters for installing engine simulators for different examined variants

Variant No.	Wing cross-section on relative span 0.383				Wing cross-section on relative span 0.65			
	$\bar{X}_{nozzle}$	$\bar{Y}_{axis}$	$\phi_{install}$, degrees	$\beta_{nacelle}$, degrees	$\bar{X}_{nozzle}$	$\bar{Y}_{axis}$	$\phi_{install}$, degrees	$\beta_{nacelle}$, degrees
10	−0.22	−0.3	−1.5	0	−0.265	−0.353	−2.5	0
11	−0.15	−0.3	−1.50	0	−0.18	−0.353	−2.50	0
12	−0.18	−0.3	−1.50	0	0.217	−0.353	−2.5	0
3a	−022	−0.26	−1.5	0	0.265	−0.32	−2.5	0

Table 5

Parameters for installing engine simulators for different examined variants

Variant No.	Wing cross-section on relative span 0.383				Wing cross-section on relative span 0.65			
	$\bar{X}_{nozzle}$	$\bar{Y}_{axis}$	$\phi_{install}$, degrees	$\beta_{nacelle}$, degrees	$\bar{X}_{nozzle}$	$\bar{Y}_{axis}$	$\phi_{install}$, degrees	$\beta_{nacelle}$, degrees
14	–0.214	–0.287	–1.5	0	–0.257	–0.366	–2.5	0
15	–0.214	–0.26	–1.50	0	–0.257	–0.32	–2.50	0

For design reasons, the closest position of the engines of a short take-off and landing turbojet aircraft was determined at the following relative parameters of installing the engines for height: the internal engine $\bar{Y}_{axis} = 0.26$ and the external engine $\bar{Y}_{axis} = 0.32$. These positions for height relative to the wing are accepted as the minimum possible arrangements to study the model with the working TJTE simulators.

Under a take-off mode, when extending the internal ($\bar{Y}_{axis} = 0.22$) and external ($\bar{Y}_{axis} = 0.267$) engine simulator, the increase in the distance from the wing to the engine simulator's axis from $\bar{Y}_{axis} = 0.26$ to $\bar{Y}_{axis} = 0.32$ reduces the increment of the lift force from the jet's blowing. This can be seen at the linear section of the dependence of a lift force coefficient on the angle of attack $C_y(\alpha)$ by $\Delta C_{y\,\max} = 0.5$ and at the maximum angle of attack $\Delta C_{y\,\max} = 0.38$.

Fig. 5 shows a change in the lift force coefficient due to the relative height of the position of the axis of the internal engine simulator under an aircraft landing approach mode. The decrease in the coefficient of the maximum lift force is due to the fact that at a decrease in the distance from the wing to the engine axis a part of the jet, which is not covered by flaps, increases, and, accordingly, the effective angle of the jet deviation decreases. Consequently, the effect of supercirculation decreases. This reduction in the coefficient of the maximum lift force leads to an increase in the landing approach speed by 8 km/h.

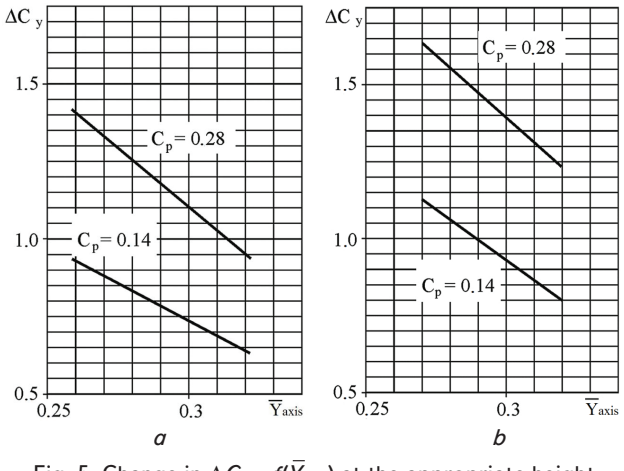

Fig. 5. Change in $\Delta C_y = f(\bar{Y}_{axis})$ at the appropriate height of the external engine simulator of 0.321 and 0.393, δ_{flap}=60°: *a* – α=8°; *b* – $\alpha = \alpha_{max}$

When the nozzles of the simulators are shifted closer to the wing, at a fixed angle of attack α=8°, there is a slight decrease in the carrying properties of the wing (Fig. 6). Studies show that the decrease in the «extension» of nacelles leads to an increase in the aircraft drag and in the resistance of interference, especially at the cruising Mach numbers [27]. Based on the results of investigating the model in the cruising configuration with the flow-through nacelles, the estimated studies at M=0.75, and the design development of the layout, we shall refine the nacelle position in terms of their «extensions».

Fig. 7, 8 show the effect of the wedge angle of the engine simulators on the carrying wing characteristics. Changing the wedge angle from –1.5° to zero reduces the lift force coefficient by ΔC_y=0.2 under a landing approach mode with flaps deflected at 60°.

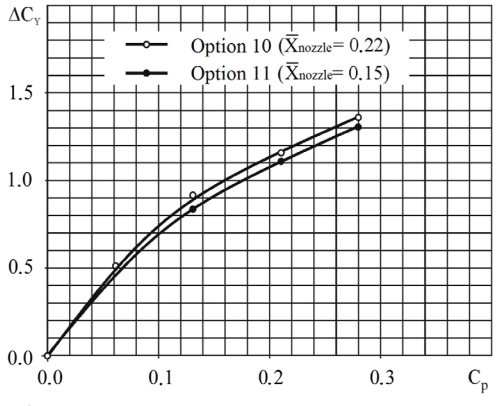

Fig. 6. The effect of power plant simulators extension at an increment in the lift force coefficient due to the blowing factor (4 TJTEs are in operation, δ_{flap} = 60°, α = 8°, M = 0.12)

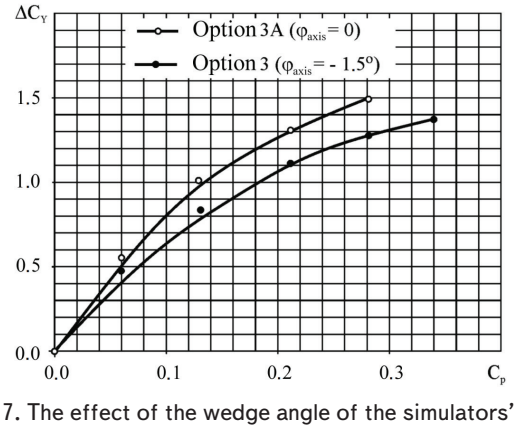

Fig. 7. The effect of the wedge angle of the simulators' axis at an increment in the lift force coefficient due to the blowing factor (4 TJTEs are in operation, δ_{flap} = 60°, α = 8°, M = 0.12)

By subordinating the layout of the engine and wing nacelles to the principle of obtaining a significant increase in the lift force, it is necessary to ensure the minimum effect of such a layout on the aircraft drag in the cruising configuration.

Assessment of the total external resistance of the airframe elements to the aircraft drag in the cruising configuration is based on the results of testing the model with the flow-through nacelles and without nacelles' rims.

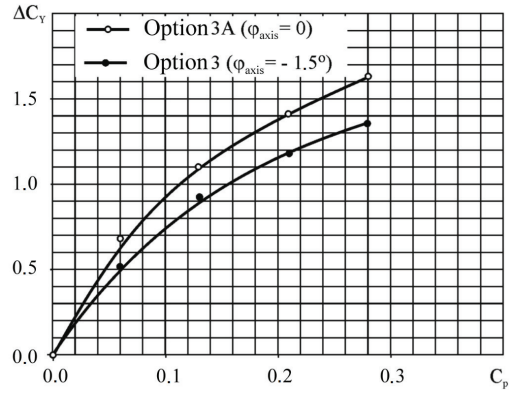

Fig. 8. The effect of the wedge angle of the simulators' axis at an increment in the lift force coefficient due to the blowing factor (4 TJTEs are in operation, $\delta_{flap}=60°$, α_{max}, $M=0.12$)

The external resistance of the fan and gas-generated contours, pylons, internal resistance of nacelle ducts $C_{x\,nacelle}$ and the interference of the layout of four nacelles, as well as the airframe, were taken into consideration. It is based on the following expression:

$$C_{x\,nacelle}=S_{wing}\Big/\left(n\cdot S_{mid\text{-}section\ nacelle}\right)\cdot\left(C_{x1}-C_{x2}\right), \quad (1)$$

where S_{wing} is the wing area of an aircraft; n is the number of engines; $S_{mid\text{-}section\ nacelle}$ is the engine nacelle midline area; C_{x1} is the drag factor of the model of an aircraft with the flow-through nacelles of the engines; C_{x2} is the drag factor of the model of an aircraft without nacelles and pylons.

6. Studying the effect of TJTE jet temperatures on the wing and mechanization

The object of our analysis is the jet stream of a TJTE, interacting with the wing of the aircraft and its mechanization in the landing configuration. We have considered the interaction between a jet stream from a TJTE and the wing of the aircraft with fully released mechanization ($\delta_{flap}=60°$) at a different distance of the engine axis relative to the mid-wing plane, at different speeds and incident flow angles. In addition, we have considered separately jets without a wing, and to analyze its structure.

The calculations include the following assumptions:

– the impact of the engine pylon on the jet is not taken into consideration;

– only a wing with the mechanization released and the engines were considered, the impact of the fuselage and other nodes of the aircraft was not considered;

– heat transfer through rigid walls is not considered.

The aircraft estimated flight modes have been investigated:

1) mode «Take-off» (TO), at $M=0.082$ (100 km/h), $H=0$, ISA (separately for a jet stream);

2) mode «0.4·Maximum Continuous» (0.4·MC) at $M=0.163$ (200 km/h), $H=300$ m, ISA (for all cases);

3) mode «0.4·MC» at $M=0.163$, $H=300$ m, ISA, $a=10°$ (for a model with the wing);

4) mode «TO» at $M=0.163$, $H=300$ m, ISA (going to circle 2, for all cases);

5) mode «0.4·MC» at $M=0.245$ (300 km/h), $H=300$ m, ISA (for all cases);

6) mode «0.4·MC» at $M=0.245$, $H=300$ m, ISA, $a=10°$ (for a model with the wing).

The values of the gas dynamics parameters of the first and second engine circuits:

1) mode «TO», $M=0.082$, $H=0$, ISA: $G_{gas}=265.1$ kgf, $G_{1K}=46.77$ kgf, $G_{2K}=218.32$ kgf, $T_{LPT}=719.04$ °C, $t^*_{C2}=59.12$°C;

2) mode «TO», $M=0.163$, $H=300$ m, ISA: $G_{gas}=262.53$ kgf, $G_{1K}=46.19$ kgf, $G_{2K}=216.34$ kgf, $T_{LPT}=719.36$ °C, $t^*_{C2}=58.62$°C;

3) mode «0.4·MC», $M=0.63$, $H=300$ m, ISA: $G_{gas}=157.6$ kgf, $G_{1K}=28.43$ kgf, $G_{2K}=128.57$ kgf, $T_{LPT}=484.58$ °C, $t^*_{C2}=33.73$ °C;

4) mode «0.4·MC», $M=0.245$, $H=300$ m, ISA: $G_{gas}=164.18$ kgf, $G_{1K}=28.65$ kgf, $G_{2K}=135.53$ kgf, $T_{LPT}=481.5$ °C, $t^*_{C2}=34.84$°C.

The calculations were carried out using the ANSYS CFX Release 14.0 software suite. The computational grid was built in the ICEM software using blocks; it consists of 9.2 million hexagonal elements.

The Shear Stress Transport turbulence model was used to more accurately calculate the boundary layer, with the Viscous Work Term enabled, to account for the heating of gas at viscous friction.

The Gama Theta Model of transient turbulence was applied. The calculation was carried out in a Double Precision mode.

In the first calculations, the jet stream from the engine without a wing with mechanization was computed, to determine the structure of the jet, to estimate the temperature at different cross-sections, and at different distances from the engine nozzle. Separately, we considered a take-off mode for the jet stream.

In subsequent calculations, the model was added with a mechanization wing and a second engine. In all estimated cases, the mechanization was maximally deviated ($\delta x_{element}=60°$, landing configuration). An engine model (Fig. 9) and a wing layout model with engines (Fig. 10) were built to perform calculations. The layout of the engines under the wing is shown in Fig. 11.

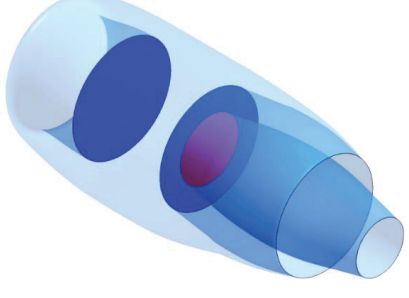

Fig. 9. General view of the engine model

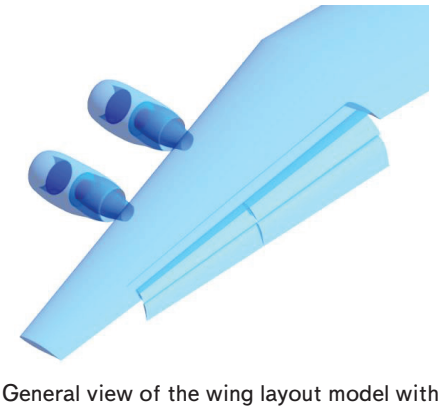

Fig. 10. General view of the wing layout model with engines

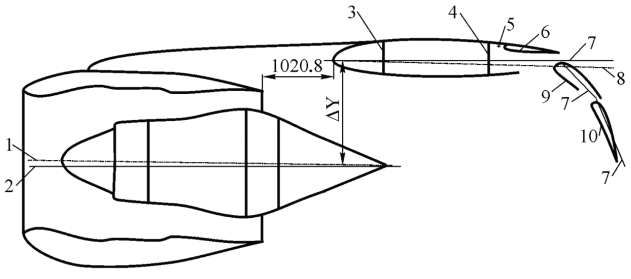

Fig. 11. Schematic of engine layout under the wing: 1 — engine axis; 2 — a line parallel to the construction plane of the wing; 3 — the first wing longeron; 4 — the second wing longeron; 5 — the spoiler axis of rotation; 6 — the spoiler theoretical contour; 7 — the construction plane of the wing, parallel to the construction plane of the fuselage; 8 — the surface of the chords; 9 — the theoretical contour of the main link of the flap; 10 — the theoretical contour of the tail link of the flap

The calculation results are demonstrated in Fig. 12–19.

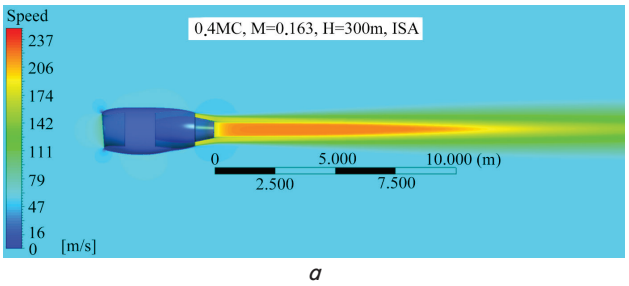

a

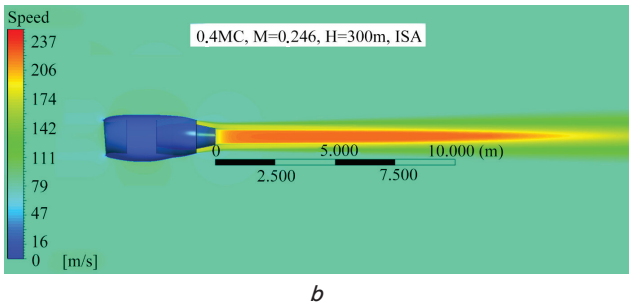

b

Fig. 12. Velocity field of the engine jet stream in the longitudinal cross-section, at different modes of operation of the engine, at different speeds of the incident flow: *a* — Mode «0.4·MC», M=0.163, H=300 m, ISA; *b* — Mode «0.4·MC», M=0.246, H=300 m, ISA

The parameters of the engine jet stream under the influence of the wing with the released mechanization have been calculated.

The distance from the engine axis to the front-edge cross-section (FEC) is ΔX=1,235 mm, the turning angle of the engine relative to FEC is $\Delta\gamma$=+1.5°.

The temperature on the outer surface of the flaps varies slightly.

Calculate the engine jet stream under the influence of the wing with the released mechanization. The distance from the engine axes to FEC is ΔX=1,235 mm, the turning angle of the engines relative to FEC is $\Delta\gamma$=−3°.

The following estimated mode is investigated: «0.4·MC», M=0.163, H=300 m, ISA.

The temperature range was increased to 400 °C.

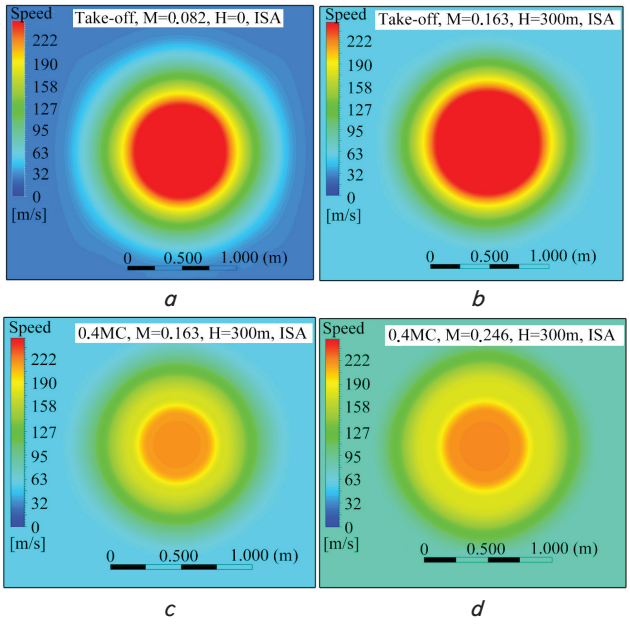

a *b*

c *d*

Fig. 13. Velocity field of the engine jet stream in the cross-section of the flap rear edge: *a* — Mode «TO», M=0.082, H=0 m, ISA; *b* — Mode «TO», M=0.163, H=300 m, ISA; *c* — Mode «0.4·MC», M=0.163, H=300 m, ISA; *d* — Mode «0.4·MC», M=0.246, H=300 m, ISA

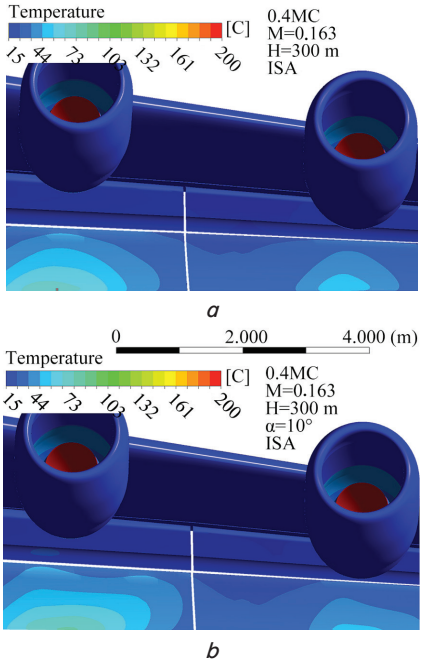

a

b

Fig. 14. Temperature field on the surface of the flaps at different angles of attack: *a* — Mode «0.4·MC», M=0.163, H=300 m, ISA, α=0°; *b* — Mode «0.4·MC», M=0.163, H=300 m, ISA, α=10°

Our analysis reveals that a given scheme of the mutual arrangement of the aircraft engine and wing does not affect the flow around the wing in the cruising configuration, which improves its characteristics.

At low speeds, by optimizing the mutual arrangement «wing-engine», it is possible to ensure a continuous «force» turn of the flow in the configuration of the flaps δ_{flap}=60°, thereby enabling landing on the runway with a length of 600–800 m.

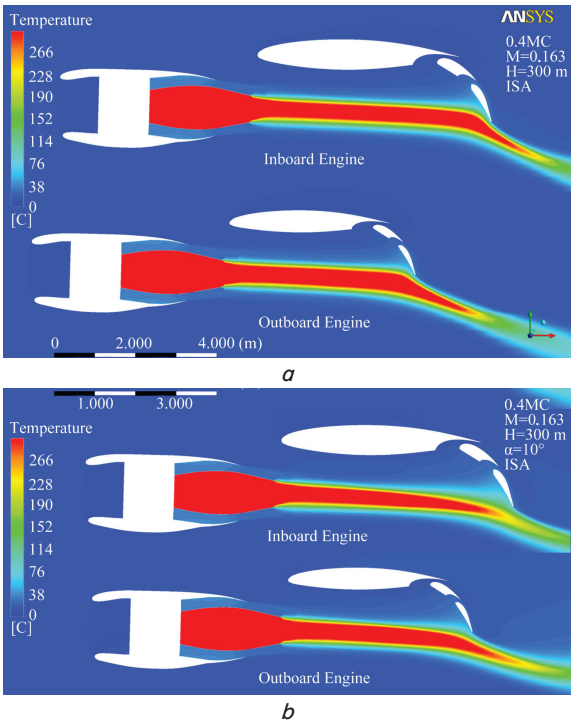

Fig. 15. Temperature field in the longitudinal cross-section at different angles of attack: *a* – Mode «0.4·MC», $M=0.163$, $H=300$ m, ISA, $\alpha=0°$; *b* – Mode «0.4·MC», $M=0.163$, $H=300$ m, ISA, $\alpha=10°$

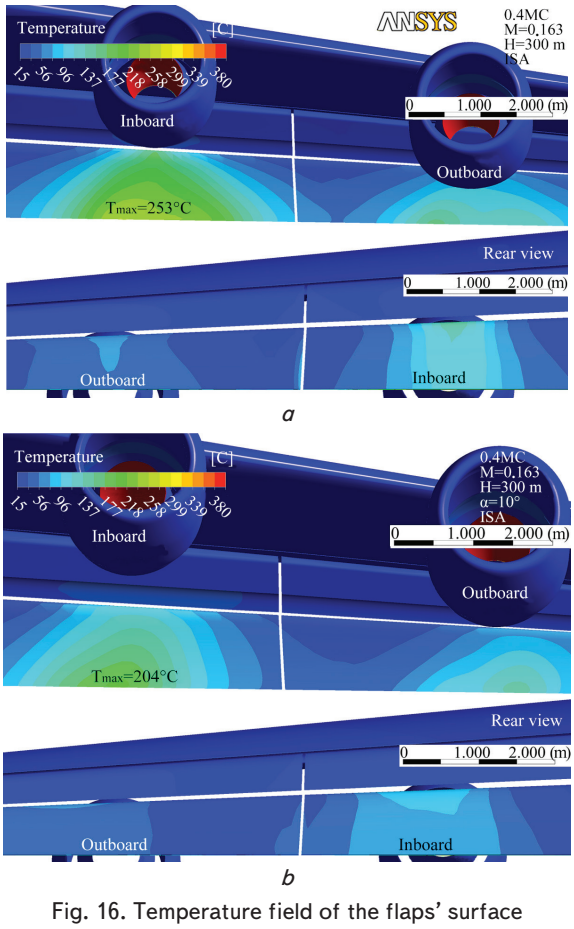

Fig. 16. Temperature field of the flaps' surface at different angles of attack: *a* – Mode «0.4·MC», $M=0.163$, $H=300$ m, ISA, $\alpha=0°$; *b* – Mode «0.4·MC», $M=0.163$, $H=300$ m, ISA, $\alpha=10°$

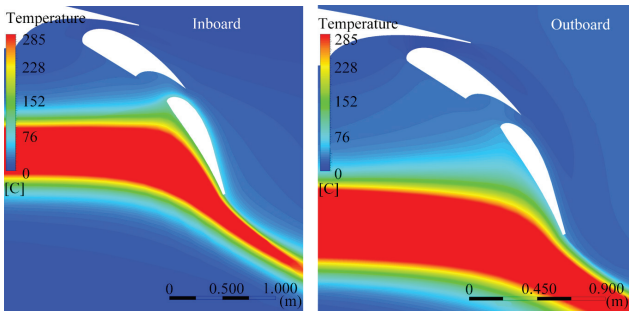

Fig. 17. The effect of mechanization on the field of temperatures at $\alpha=0°$: *a* – internal engine; *b* – external engine

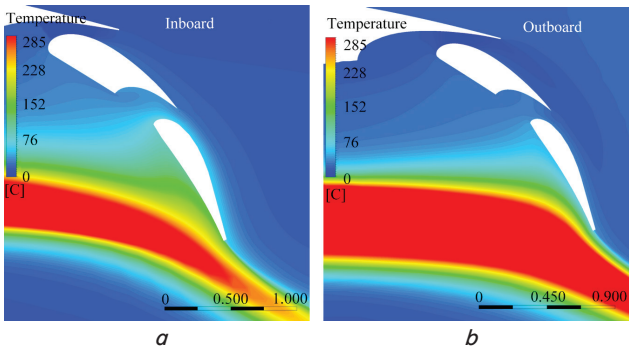

Fig. 18. The effect of mechanization on the field of temperatures at $\alpha=10°$: *a* – internal engine; *b* – external engine

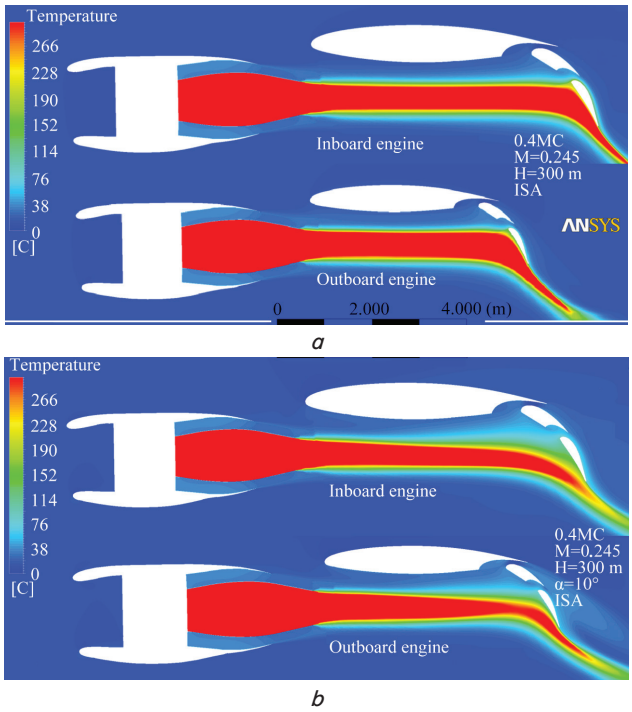

Fig. 19. Temperature field in the longitudinal cross-section at different angles of attack: *a* – Mode «0.4·MC», $M=0.245$, $H=300$ m, ISA, $\alpha=0°$; *b* – Mode «0.4·MC», $M=0.245$, $H=300$ m, ISA, $\alpha=10°$

There should also be the optimization of the TJTE air intake in order to obtain the loss of full pressure at the inlet not exceeding 1.5 %.

7. Discussion of results of studying the flight-technical characteristics of a short take-off and landing aircraft

The result of the numerical study of the parameters of the flow of gas and air flows is the determined mutual arrangement of the TJTE and the wing, which makes it possible to obtain the maximum increase in the lift force due to the «forced» turning of the engine jet streams.

The reported results have confirmed that the jet stream does not exert an impact on the aircraft drag in the cruising configuration (Fig. 12–19). Our analysis of the parameters of the aircraft's integrated energy systems demonstrates:

– a significant reduction in gas-dynamic losses along the power plant tract;

– a reduction in operating costs';

– achieving the required aircraft noise indicators on the ground now and for the future.

The calculation of the TJTE jet stream shows that at low speeds and on the ground the mixing of hot and cold jets occurs faster than at high flight speeds (Fig. 12). At low flight speeds, the jet stream expands faster than at high flight speeds (Fig. 13).

At low flight speeds, the temperature on the outer surface of the flaps changes slightly (Fig. 14). The temperature field in the longitudinal cross-section at different angles of attack has little effect on the gas dynamics of the flow around the flaps (Fig. 15, 16). The deviation of wing mechanization has a significant impact on the distribution of the temperature field at $\alpha=0°$ (Fig. 17). In the cross-section of the tail section of the flap, in the zone of its position in a fully released state, the gas temperature is 176–444 °C (Fig. 18).

An analysis of the results of studying the temperature fields reveals that the inclination angle of the flaps strongly affects the course and level of turbulence in the jet. Due to the interaction of the jet with the end vortexes coming off the flaps, the jet deforms, there is an azimuth heterogeneity in the distribution of the parameters of the flow in the cross-sections of the jet [27]. The energy of the flow turbulence increases by 1.5–2 times compared to the gas flow, which does not get on the flaps.

Fig. 19 shows that the hot jet of the first circuit and the cold jet of the second circuit do not have time to mix before reaching the mechanization zone. Therefore, the cold jet isolates the hot jet from interaction with the flap. However, due to viscous friction and the ratio of air consumption through the crevices of the mechanization, in a certain position of the engines ($\Delta X_{internal} \leq 830$ mm, $\Delta X_{external} \leq 765$ mm) the isolating part of the cold jet completely goes into the gap between the end and the main link of the flap. The non-isolated hot jet comes into contact with the tail link of the flap and raises the surface temperature of the flap in the contact area to 400 °C.

We have identified those tail sections of the flap that require special technological execution to operate at temperatures of up to 400 °C.

The advancement of this study may be the use of other models of turbulence in calculating the process of the outflow of the hot jet and the interaction with the flap. The main difficulty of verifying a mathematical model is the experimental part.

8. Conclusions

1. We have analyzed basic requirements for the flight characteristics of a short take-off and landing aircraft. The aircraft with a wing sweep of $\chi_{1/4}=14–20°$ with an elongation of $\lambda=9–109–10$ was investigated. A wing with such an elongation may be the most optimal in terms of weight in the case of applying supercritical profiles, as well as modern metallic and compositional materials. For the aircraft, a unique aerodynamic layout of PP and a highly mechanized wing has been designed, which makes it possible to obtain a very high lift force, necessary for the short takeoff and landing.

2. We have substantiated the characteristics of the transport aircraft and compared them with European projects. The domestic project of the aircraft exceeds, in terms of performance, the capabilities of the Il-76 family and the European A400M aircraft and is close to the capabilities of the heavy transport aircraft S-17, which has twice the take-off weight and three times the price.

In terms of its dimensions and take-off mass, the medium transport aircraft equipped with TJTE approaches the European Airbus Military A400M aircraft and, based on a series of basic flight-technical characteristics, significantly outperforms it.

3. Comprehensive studies have been carried out into the effect of the jets from operating simulators on the aerodynamic characteristics of the mechanized model of the aircraft. It has been established that the scheme of the mutual arrangement of the engine and wing of the aircraft does not affect the flow around the wing in the cruising configuration, which improves its characteristics.

4. The effect of the temperature of the TJTE jet stream on the wing and its mechanization has been investigated. The hot jet of the first circuit and the cold jet of the second circuit do not have time to mix before reaching the mechanization zone. We have identified those zones in the tail section of the flap that require special technological execution to operate at temperatures of up to 400 °C. At the same time, the temperature on the outer surface of the flaps varies slightly.

References

1. Flying in 2050? Available at: http://www.academie-air-espace.com/upload/doc/ressources/CP-2050-VOLUME2.pdf
2. Grebenikov, A. G. (2006). Metodologiya integrirovannogo proektirovaniya i modelirovaniya sbornyh samoletnyh konstruktsiy. Kharkiv: Nats. aerokosm. un-t «KhAI», 532.
3. Zhitomirskiy, G. I. (2005). Konstruktsiya samoletov. Moscow: Mashinostroenie, 406.
4. Petersson, O., Daoud, F. (2012). Multidisciplinary optimization of aircraft structures with respect to static and dynamic aeroelastic requirements. Deutscher Luft- und Raumfahrtkongress. Berlin, 1–7.
5. Gagnon, H., Zingg, D. W. (2014). High-fidelity Aerodynamic Shape Optimization of Unconventional Aircraft through Axial Deformation. 52nd Aerospace Sciences Meeting. doi: https://doi.org/10.2514/6.2014-0908
6. Loginov, V. V. (2009). Kompleksniy podhod po formirovaniyu tehnicheskogo oblika silovoy ustanovki, integriruemoy v planer, pri sinteze letatel'nogo apparata. Intehrovani tekhnolohiyi ta enerhozberezhennia, 2, 88–99.

7. Pezhman, M. (2013). Effects of engine placement and morphing on nonlinear aeroelastic behavior of flying wing aircraft. Atlanta: Georgia Institute of Technology, 133.
8. Vasil'ev, V. I., Lavruhin, G. N., Lazarev, V. V., Noskov, G. P., Talyzin, V. A. (2014). Eksperimental'noe issledovanie harakteristik integral'noy silovoy ustanovki samoleta tipa «letayushchee krylo». Uchenye zapiski TSAGI, 45 (3), 45–52.
9. Lyu, Z., Martins, J. R. R. A. (2015). Aerodynamic Shape Optimization of an Adaptive Morphing Trailing-Edge Wing. Journal of Aircraft, 52 (6), 1951–1970. doi: https://doi.org/10.2514/1.c033116
10. Zlenko, N. A., Kursakov, I. A. (2015). Optimizatsiya geometrii uzla podveski motogondoly pod krylom passazhirskogo samoleta na osnovanii chislennyh raschetov s ispol'zovaniem uravneniy RANS. Uchenye zapiski TSAGI, 46 (5), 21–38.
11. Wilhelm, R. (2005). An inverse design method for engine nacelles and wings. Aerospace Science and Technology, 9 (1), 19–29. doi: https://doi.org/10.1016/j.ast.2004.09.002
12. Babulin, A. A. (2005). Primenenie programmnogo kompleksa «Sprut» dlya issledovaniya voprosov mestnoy aerodinamiki passazhirskogo samoleta. Materialy XVI shkoly-seminara «Aerodinamika letatel'nyh apparatov». Zhukovskiy: TSAGI, 14–15.
13. Anisimov, K. S., Kazhan, E. V., Kursakov, I. A., Lysenkov, A. V., Savel'ev, A. A. (2016). Chislennoe issledovanie vneshney aerodinamiki dvigatelya v ramkah metodiki mnogodistsiplinarnoy optimizatsii. Materialy XXVII nauch.-tehn. konf. po aerodinamike. Zhukovskiy: TSAGI, 33–34.
14. Fomin, V. M., Hozyaenko, N. N., Shipovskiy, G. N. (2005). Osobennosti obtekaniya komponovki regional'nogo samoleta s dvigatelyami na fyuzelyazhe. Materialy XVI shkoly-seminara «Aerodinamika letatel'nyh apparatov». Zhukovskiy: TSAGI, 101–103.
15. Bragin, N. N., Gubanova, M. A., Gurevich, B. I., Karas', O. V., Kovalev, V. E., Skomorohov, S. I., Chernavskih, Yu. N. (2009). Aerodinamicheskoe proektirovanie i opredelenie harakteristik grazhdanskogo samoleta s upravlyaemym vektorom tyagi. Materialy XX shkoly-seminara «Aerodinamika letatel'nyh apparatov». Zhukovskiy: TSAGI, 34–35.
16. Petrov, A. B., Tret'yakov, V. F. (2015). Vliyanie struy reaktivnyh dvigateley bol'shoy stepeni dvuhkonturnosti na aerodinamicheskie harakteristiki mehanizirovannogo kryla. Uchenye zapiski TSAGI, 46 (7), 1–10.
17. Gubanov, A. A., Gusev, D. Yu. (2014). Issledovaniya integral'noy komponovki letatel'nogo apparata s pryamotochnym dvigatelem. Uchenye zapiski TSAGI, 45 (3), 12–19.
18. Kornushenko, A. V., Chernyshova, S. M., Yastrebov, Yu. G., Bytsko, N. S. (2010). Issledovaniya vliyaniya modifikatsii elementov modeli regional'nogo samoleta na aerodinamicheskie harakteristiki modeli. Materialy XXI nauch.-tehn. konf. po aerodinamike. Zhukovskiy: TSAGI, 101–102.
19. Gorbunov, V. G., Zhelannikov, A. I., Dets, D. O., Setukha, A. V. (2012). Flow over aircraft simulation by using the discrete singularity method. Nauchniy vestnik MGTU GA, 177, 10–13.
20. Gu, X., Ciampa, P. D., Nagel, B. (2016). High fidelity aerodynamic optimization in distributed overall aircraft design. 17th AIAA/ISSMO Multidisciplinary Analysis and Optimization Conference. doi: https://doi.org/10.2514/6.2016-3508
21. Bragin, N. N., Bolsunovskiy, A. L., Buzoverya, N. P., Gubanova, M. A., Skomorohov, S. I., Hozyainova, G. V. (2013). Issledovaniya po sovershenstvovaniyu aerodinamiki vzletno-posadochnoy mehanizatsii kryla passazhirskogo samoleta. Uchenye zapiski TSAGI, 44 (4), 1–14.
22. Bui, T. T. (2016). Analysis of Low-Speed Stall Aerodynamics of a Swept Wing with Seamless Flaps. 34th AIAA Applied Aerodynamics Conference. doi: https://doi.org/10.2514/6.2016-3720
23. Balabuev, P. V., Bychkov, S. A., Grebenikov, A. G., Zheldochenko, V. N., Kobylyanskiy, A. A., Myalitsa, A. K. et. al. (2003). Osnovy obshchego proektirovaniya samoletov s gazoturbinnymi dvigatelyami. Ch. 1. Kharkiv: «KhAI», 454.
24. Braddon, D., Lawrence, P. (1998). The Strategic Case for A400M. Aerospace Research Group, Faculty of Economics and Social Science. UWE Bristol, BS16 1QY.
25. Epifanov, S. V., Pehterev, V. D., Ryzhenko, A. I., Tsukanov, R. Yu., Shmyrev, V. F. (2011). Proektirovanie sistem silovyh ustanovok samoletov. Kharkiv: «KhAI», 511.
26. Kiva, D. S., Grebenikov, A. G. (2014). Nauchnye osnovy integrirovannogo proektirovaniya samoletov transportnoy kategorii. Ch. 1, 2. Kharkiv: Nats. aerokosm. un-t im. N. E. Zhukovskogo «KhAI», 439, 376.
27. Lyubimov, D. A. (2013). Investigation of the effect of a pylon and a wing with flaps on the flow within an exhaust jet of a double-flow turbojet engine by a simulation method for large eddies. High Temperature, 51 (1), 111–127. doi: https://doi.org/10.1134/s0018151x12050100